European Journal of Medicinal Chemistry 49 (2012) 271–278

Contents lists available at SciVerse ScienceDirect

European Journal of Medicinal Chemistry

journal homepage: http://www.elsevier.com/locate/ejmech

Original article

Synthesis and biological evaluation of quinazoline and quinoline bearing 2,2,6,6-tetramethylpiperidine-N-oxyl as potential epidermal growth factor receptor(EGFR) tyrosine kinase inhibitors and EPR bio-probe agents

Siyuan Li [a], Chunying Guo [a], Xianqiang Sun [c], Yaozong Li [c], Hongli Zhao [a], Dongmei Zhan [a], Minbo Lan [a,b,*], Yun Tang [c,**]

[a] Shanghai Key Laboratory of Functional Materials Chemistry, and Research Centre of Analysis and Test, East China University of Science and Technology, Meilong Road 130, Shanghai 200237, PR China
[b] State Key Laboratory of Bioreactor Engineering, East China University of Science and Technology, Shanghai 200237, PR China
[c] Department of Pharmaceutical Science, School of Pharmacy, East China University of Science and Technology, Shanghai 200237, PR China

ARTICLE INFO

Article history:
Received 8 September 2011
Received in revised form
8 January 2012
Accepted 10 January 2012
Available online 24 January 2012

Keywords:
EGFR
Inhibitor
Bio-probe
Free radical
Quinazoline

ABSTRACT

4-anilinoquinazoline and 4-anilinoquinoline scaffolds bearing a 2,2,6,6-tetramethylpiperidine-N-oxyl(TEMPO) have been synthesized and evaluated for their ability to inhibit EGFR tyrosine kinase and A431 cell lines. Compared to their corresponding parent compounds, all of the new compounds bearing a TEMPO showed more efficient inhibition for EGFR and A431 cells. Furthermore, we have proved that these molecules bearing a TEMPO can exactly get into A431 cells exerting inhibitory effect that may be used for EPR detecting. In our docking model, quinazolines bearing a TEMPO on either 6- or 3-positions took different linking modes according to EGFR crystal structure. In contrast to their parent compounds, these new TEMPO-derived analogues possessed compatible inhibitory effect that might be useful as potential EGFR inhibitors and as EPR bio-probes.

1. Introduction

Cancer and carcinogenesis are complex pathology and multifactor processes that require the accumulation of several biochemical alterations in a single cell. All complex diseases are most likely ascribed to multifactorial effect, and these factors may interact with each other, hence inducing interdependent biological changes in a single cell over a period of time. The interaction of the multifactorial effects used to aggravate worsening of cancer. To solve the extraordinary complexity of cancer and provide excellent therapeutic drugs, several researchers have made their R&D efforts to discover new multifunctional drugs which are able to interfere with multiple altered pathways [1,2].

The human EGFR is a transmembrane glycoprotein, which consists of a single polypeptide chain of 1186 amino acids [3,4]. It is also a receptor tyrosine kinase (RTK) that is catalytically active and under tight regulatory control. This receptor belongs to the ErbB/HER family of ligand-activated RTKs, which includes four structurally similar members EGFR/HER1, ErbB2/HER2, ErbB3/HER3 and ErbB4/HER4 [5]. EGFR and its family members play crucial roles in regulating a number of cellular processes including cell proliferation, survival and migration [6] and dysregulation of their activity is, therefore, strongly associated with malignancy of numerous types of human tumors [7]. The involvement of increased and/or aberrant EGFR activity in human cancers is well investigated [8,9], while cancer patients with altered EGFR activity tend to have a more aggressive disease, associated with a poor prognosis [5]. Considering EGFR is a rational target for anti-tumor strategies, one of the most important methods to inhibit EGFR is to block tyrosine kinase at ATP-binding site in cytoplasmic domain by small-molecule inhibitors. The representative frame of inhibitor is 4-anilinoquinazolines, such as gefitinib (ZD-1839; Iressa) and lapatinib (GW2016; Tykerb) approved in the U.S. by the FDA (Fig. 1).

* Corresponding author. Shanghai Key Laboratory of Functional Materials Chemistry, and Research Centre of Analysis and Test, East China University of Science and Technology, Meilong Road 130, Shanghai 200237, PR China. Tel.: +86 21 64253574; fax: +86 21 64252947.
** Corresponding author. Tel.: +86 21 64251052; fax: +86 21 64253651.
E-mail addresses: minbolan@ecust.edu.cn (M. Lan), ytang234@ecust.edu.cn (Y. Tang).

0223-5234/$ – see front matter © 2012 Elsevier Masson SAS. All rights reserved.
doi:10.1016/j.ejmech.2012.01.021

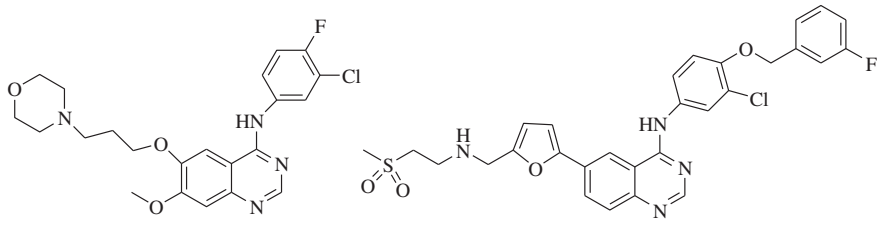

Fig. 1. Structure of Gefitinib and Lapatinib.

However, just inhibiting EGFR is not enough to eradicate tumors, that is to say mono-therapeutic molecule is not sufficient for ameliorating symptom. The limited anti-tumor efficacy and tools make researchers try their utmost to find other better methods to treat cancer. For example, based on multifunctional concept or multitarget-directed drug design strategy, some researchers have designed and synthesized several molecules which would not only target EGFR but also intervene with alteration of cell function, which have achieved good curative effect [10–13].

Nowadays, with the development of cancer detection techniques, electron paramagnetic resonance (EPR) spin labeling using paramagnetic molecules such as nitroxide free radicals have gained conspicuous attention. Therefore, we get interested in nitroxide compound which has been found to be an available agent and its application has achieved great progress. First of all, as we know, nitroxides have been studied as a treatment for existing tumors [14–17]. Secondly, nitroxides are able to act as an EPR functional bio-probe reagent [18–20]. Especially, EPR spin labeling techniques provide a convenient method to detect cancers on-line. Therefore we believe that EGFR inhibitors such as 4-anilinoquinazoline or 4-anilinoquinoline bearing a nitroxyl group are favorable to improve anticancer potency, and nitroxide compounds may be useful as a bio-probe for EPR spin labeling of EGFR overexpressing cancers.

For the present report, we choose 6-amino-4-anilinoquinazoline and 3-carboxyl-4-anilinoquinoline, which possess similar skeleton with Gefitinib, as our compound models. The 6-amine and 3-carboxyl are active groups which could be conjunct with other small molecular chains. It means the two compound models are efficient lead compounds for our purpose: enable certain anticancer effect of EPR bio-probe agent (Fig. 2).

In this paper, a series of compounds were designed and synthesized to show inhibitory activities against EGFR and A431 cells. These compounds were further confirmed to enter cells, which were possible to be used as EPR bio-probe agents.

2. Chemistry

Compounds **1a**–**c** and **2a**–**c** were prepared according to the method of Tsou et al. [21] and Wissner et al. [22]. Compounds **3a**–**c** were synthesized by condensing with **1a**–**c** and 4-carboxy-2,2,6,6-tetramethylpiperidine-N-oxyl (**4-COOH-TEMPO**). Similarly, compounds **4a**–**c** were obtained by condensing with **2a**–**c** and 4-amino-2,2,6,6-tetramethylpiperidine-N-oxyl (**4-NH$_2$-TEMPO**) using EDC and HOBt in different solvents. (Scheme 1).

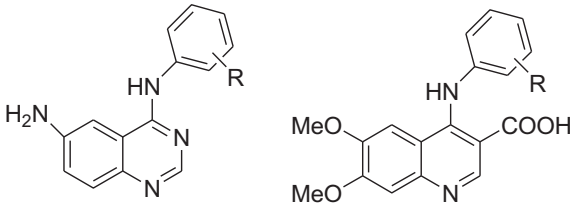

Fig. 2. Structure of 6-amino-4-anilinoquinazoline and 3-carboxyl-4-anilinoquinoline.

3. Results and discussion

3.1. EGFR kinase inhibitory assay

EGFR kinase inhibitory activity of **1a**–**c**, **2a**–**c**, **3a**–**c** and **4a**–**c** was evaluated by homogeneous time-resolved fluorescence (HTRF) KinEASE-TK assay from Cisbio according to manufacture's instruction. Gefitinib was chosen as a standard compound in kinase assay and its IC_{50} value was 7.3 nM. As showed in Table 1, series **1** and **3** showed the highest inhibitory activities among these compounds, and their IC_{50} values were 189 nM, 53 nM and 29 nM for **1a**, **1b** and **1c** while 65 nM, 31 nM and 15 nM for **3a**, **3b** and **3c**, respectively. Compounds **4a**–**c** showed the moderate inhibitory activities and **2a**–**c** displayed the lowest inhibitory activities. The IC_{50} values are different among **3a**–**c**, because halogen is different in 4-aniline. Compound **3c** is the most potent one due to the strongest electronegativity of fluorine in 4-aniline. For **2a**–**c,** IC_{50} values are close to 10 μM, possibly because the carboxyl in 3-position improves the hydrophilicity of whole molecular that decreases the hydrophobic interaction between ligand and EGFR protein. Furthermore, in our docking model, the docking poses of compounds **4a**–**c** were different from **2a**–**c**. A carboxyl was substituted on 3-position of quinoline in compounds **2a**–**c** which were less potent than series **4** compounds. The most possible reason is that electrostatic repulsion may happen between the carboxyl and Asp855. This can be proved in our docking study, and the nearest distance between the two carboxyls is only 3.72 Å.

In the kinase assay, compounds **3a**–**c** and **4a**–**c**, the TEMPO-derived analogues showed the enhanced potency to EGFR in contrast to their corresponding parent compounds. The inhibitory activity of compounds **3a**–**c** is much higher than **4a**–**c**, and this indirectly proved the binding mode of **3a**–**c** is much more reasonable than **4a**–**c** in our docking experiment.

3.2. In vitro cytotoxicity assay

The antiproliferative activities of **3a**–**c** and **4a**–**c** were evaluated with human epidermoid carcinoma cells (A431) comparing with **1a**–**c**, **2a**–**c** and TEMPO. The A431 cell lines were known to overexpress EGFR, which was related to abnormal activity of EGFR pathway in many carcinogenesis. Generally, the activity of inhibiting A431 cell proliferation was determined after 72 h of treatment with various concentrations (0.1–100 μM) of the tested compounds. The cell proliferation

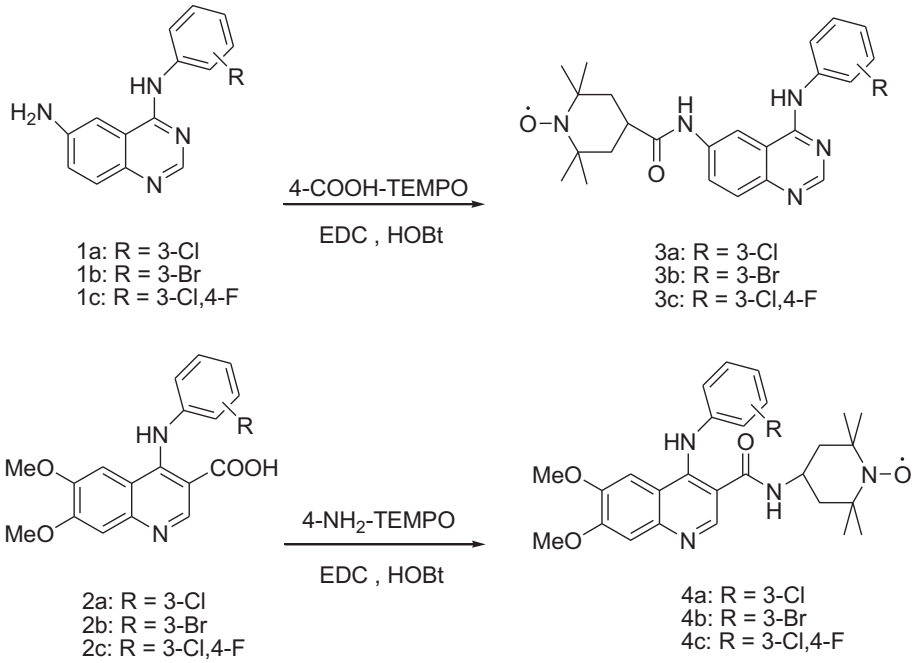

Scheme 1. Syntheses of **3a**–**c** and **4a**–**c**.

was measured by MTT assay, and the results were expressed as IC_{50} values (Table 2).

As showed in Table 2, treatment of A431 cells with compounds **1a**–**c** and **2a**–**c** made the cell proliferation decrease with IC_{50} values being 31.94 μM, 34.89 μM and 26.54 μM for **1a**–**c** and 97.85 μM, 93.99 μM and 88.83 μM for **2a**–**c**. For **2a**–**c**, the IC_{50} values are higher than **1a**–**c** possibly because compound **2a**–**c** bear a carboxyl at 3-position on quinoline ring which increases their water solubility dramatically and decreases cell permeable capacity. As expected, compounds **3a**–**c** and **4a**–**c** bearing a TEMPO appear more potent than their corresponding parent compounds against A431 cells. As reported in Table 2, IC_{50} values of compounds **3a**, **3b**, **3c** decrease 5.09 μM, 7.51 μM and 1.84 μM in contrast to **1a**, **1b**, **1c**, respectively. Extremely, IC_{50} values of compounds **4a**, **4b** and **4c** decrease 52.39 μM, 50.12 μM and 50.69 μM compared with compounds **2a**, **2b** and **2c**, respectively. A TEMPO on 3-position in quinoline ring, other than a carboxyl, might help to improve hydrophobicity to enter cells for **4a**–**c**. In parallel, we also tested TEMPO for inhibiting A431 cells, and the IC_{50} value was higher than 300 μM. To some extent, TEMPO showed anticancer activities on several cancer cell lines, but it was ineffective against A431 cell lines at our tested concentration. It seems reasonable, because TEMPO is not an EGFR inhibitor. In the assay, antiproliferative activities of some compounds were inconsistent with their kinase assay data. Especially, compounds **1a**–**c** and **3a**–**c** showed antiproliferative potency at micromole order of magnitude even though they had reasonable levels of target potency at the enzyme level. Possibly, these compounds do not possess enough cell permeable capacity.

To further illustrate the effect of free radical on cell antiproliferation, we also carried out the control experiment by combining compounds **1** and **2** series and TEMPO on A431 cells. As

Table 1
EGFR kinase inhibitory activities of **1a**–**c**, **2a**–**c**, **3a**–**c**, **4a**–**c**.

Compd	[a]Inhibitory activity at 10 μM	[a]IC_{50} (nM)
1a	98.9 ± 0.5	189 ± 18
1b	99.3 ± 0.1	53 ± 8
1c	99.5 ± 0.2	29 ± 4
2a	63.4 ± 2.1	9021 ± 124
2b	60.1 ± 1.3	8719 ± 38
2c	66.5 ± 0.7	9284 ± 231
3a	99.4 ± 0.2	65 ± 6
3b	99.4 ± 0.4	31 ± 2
3c	99.5 ± 0.3	15 ± 6
4a	88.3 ± 0.4	623 ± 79
4b	90.3 ± 1.2	342 ± 27
4c	92.8 ± 0.8	422 ± 18
Gefitinib[b]	99.6 ± 0.2	7.3 ± 0.2

[a] The values are the mean ± SD of at least two independent experiments.
[b] IC_{50} value of Gefitinib is 3.1 nM determined by Klutchko et al. [23].

Table 2
In vitro antiproliferation of compounds **1a**–**c**, **2a**–**c**, **3a**–**c**, **4a**–**c** and **TEMPO** in A431 cells.[a]

Compd	IC_{50} (μM)[b], A431
1a	31.94 ± 0.29
1b	34.89 ± 1.64
1c	26.54 ± 0.92[d]
2a	97.85 ± 0.60
2b	93.99 ± 1.81
2c	88.83 ± 1.78
3a	26.85 ± 0.38
3b	27.38 ± 1.44
3c	24.70 ± 1.02
4a	45.46 ± 2.01
4b	43.21 ± 3.41
4c	38.14 ± 2.47
Tempo	> 300[c]

[a] The values are the mean ± SD of at least three independent experiments.
[b] Concentration of compound resulting in 50% inhibition of A431 cell proliferation. The cell proliferation in A431 cells was determined by the MTT assay, after 72 h of incubation with compounds (0.1–100 μM).
[c] IC50 was not determined because less than 50% inhibition was observed at the highest tested concentration (300 μM).
[d] Reported activity in reference.IC_{50} 25–30 μM against A431 [24].

Table 3
IC_{50} (μM) of combination of compounds **1**/**2** and **TEMPO** on A431 cell antiproliferation.

Compd	TEMPO (1 eq.)	TEMPO (2 eq.)	TEMPO (5 eq.)
1a	32.54 ± 0.78	31.55 ± 1.02	32.33 ± 0.34
1b	34.43 ± 1.20	33.21 ± 0.98	33.45 ± 1.42
1c	28.51 ± 0.48	24.74 ± 1.21	26.12 ± 1.27
2a	96.65 ± 0.40	98.52 ± 0.91	97.40 ± 0.33
2b	92.21 ± 1.21	91.90 ± 1.93	92.29 ± 0.17
2c	87.55 ± 1.54	88.11 ± 2.91	87.23 ± 3.32

shown in Table 3, the potency was altered not too much even though the ratio (TEMPO/**1** or **2**) was up to 5. It clearly indicates combination TEMPO with inhibitor does not exhibit synergistic effect on antiproliferation of A431 cell lines. Conjugation inhibitor with TEMPO, only in this way, could display the more favorable antiproliferation on A431 cells as the data shown in Table 2 and Table 3. Although intracellular TEMPO does not attack a specific molecular target, it may alter the entire physicochemical characters of the molecule. Hydrophobicity, for example, is helpful in entering into cells to some extent for **4a**–**c**.

3.3. EPR detecting

Free radical like TEMPO and other small molecules can readily enter cells [25], but it is not clear that whether a molecule bearing a TEMPO such as **3c** and **4c** can enter cells. Considering compounds **3a**–**c** and **4a**–**c** are likely to be a bio-probe for cancer which needs to enter cancer cells, we tested **3c** and **4c** entering A431 cells using EPR techniques. As a result, EPR signals of intracellular **3c** and **4c** could be detected, which proved these compounds can get into cells (Fig. 3).

As shown in Fig. 3, EPR signals of **3c** and **4c** in DMSO were smoothly triple peaks. Treating A431 cells with **3c** and **4c**, removing **3c** and **4c** in the medium, **3c** and **4c** inside cells can be detected with EPR spectroscopy which displays a triple peak (**3c-cell** and **4c-cell**). Despite little higher noise in signals caused by cells in the DMSO solution, it indicated that the **3c** and **4c** were able to enter A431 cells. As we know the EGFR is characterized by three main domains: an extracellular ligandbinding domain, a transmembrane domain and a cytoplasmic domain containing the tyrosine kinase [5,25]. EGFR inhibitors must get into cytoplasmic domain to bind with tyrosine kinase. In MTT assays, **3c** and **4c** achieved favorable antiproliferation against A431 cell lines compared with **1a**–**c** and **2a**–**c**, which also proved **3c** and **4c** can enter cells. Considering kinase inhibitory activity of **3a**–**c** (IC_{50} = 65, 31, 15 nM) is comparable to **1a**–**c** (IC_{50} = 189, 53, 29 nM), compounds **3a**–**c** are more favorable to be candidates of EGFR inhibitor and bio-probes for EPR spin labeling of EGFR overexpressing cancers.

3.4. Molecular docking

Many EGFR crystal structures have been reported from previous studies [26,27]. Among all the structures, 1XKK was selected for our docking investigation because of its high resolution and the high similarity of our compounds and lapatinib in the crystal structure. Comparing the 4-anilinoquinazoline with the corresponding fragment of lapatinib in the binding pocket, all of the ligands took the rational binding pose in our study. Furthermore, the ring-O^{-1} state possesses more similar electrostatics with the radical state than the ring-OH state, thus it is reasonable to use the ring-O^{-1} state as a substitute.

Compound **3c** binds in the ATP-binding cleft in a fashion similar to what observed in other kinase-quinazoline crystal structure (Fig.4C) [26,27]. A hydrogen bond forms between the N1 of the quinazoline and the main chain NH of Met793, and the distance is 2.31 Å while the angle value is 173°. The 3-chloro-4-fluorophenylamino was deeply in the back of the ATP-binding site and makes predominantly hydrophobic interactions with the protein. Increasing this hydrophobic interaction might increase the activity slightly. That is the possible reason why **3c** was more potent towards EGFR than its corresponding ligands in series **a** and **b** in our kinase assay. The N in tetramethylpiperidine in **3c** formed a hydrogen bond with carboxyl in Asp800. The distance and the angle of this hydrogen bond were 1.84Å and 152°. Thus, we supposed that positive charged in this region might increase the activity. Compound **1c** took almost the same binding mode with compound **3c** except for the tetramethylpiperidine regions. The 1-N of quinazoline is located 1.98Å from the backbone NH of Met793, and the angle of this hydrogen bond is 164°. Detailed binding mode of compound **1c** to EGFR can be seen in Fig.4A.

Compound **4c** was another TEMPO bearing ligand with a certain activity in EGFR kinase assay. The 3-chloro-4-fluorophenylamino in compound **4c** occupied the same position as compound **3c** (Fig.4D). However, the quinazoline ring was binding differently. A hydrogen bond was formed between the N in 4-aniline and the Asp855 carboxyl. The oxygen in methoxyl of dimethoxyquinoline occupied the N1 position of the quinazoline in compound **3c**, and this oxygen in methoxyl formed a hydrogen bond with the main chain NH of Met793. An Asp855 and Met793 across binding pose formed. However, compound **2c** was binding in a different binding mode compared with the back bone of compound **4c** (Fig.4B). The dimethoxyquinoline took a 180° spin and the hydrogen bond with Met793 was broken by this rotation.

Met793 was proved to be an important residue in ligand binding [28]. Both compounds **3c** and **4c** hydrogen bonded to this residue and showed favorable biological activity for EGFR and A431 cell lines, and **3a**–**c** might be used as an inhibitor with bio-probe function. Our theoretical results were in conformity with the

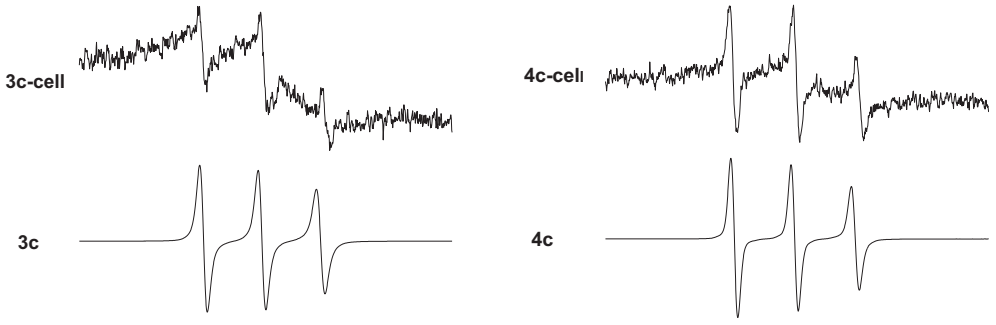

Fig. 3. The EPR signals of **3c** and **4c** in DMSO and cells, respectively.[a]

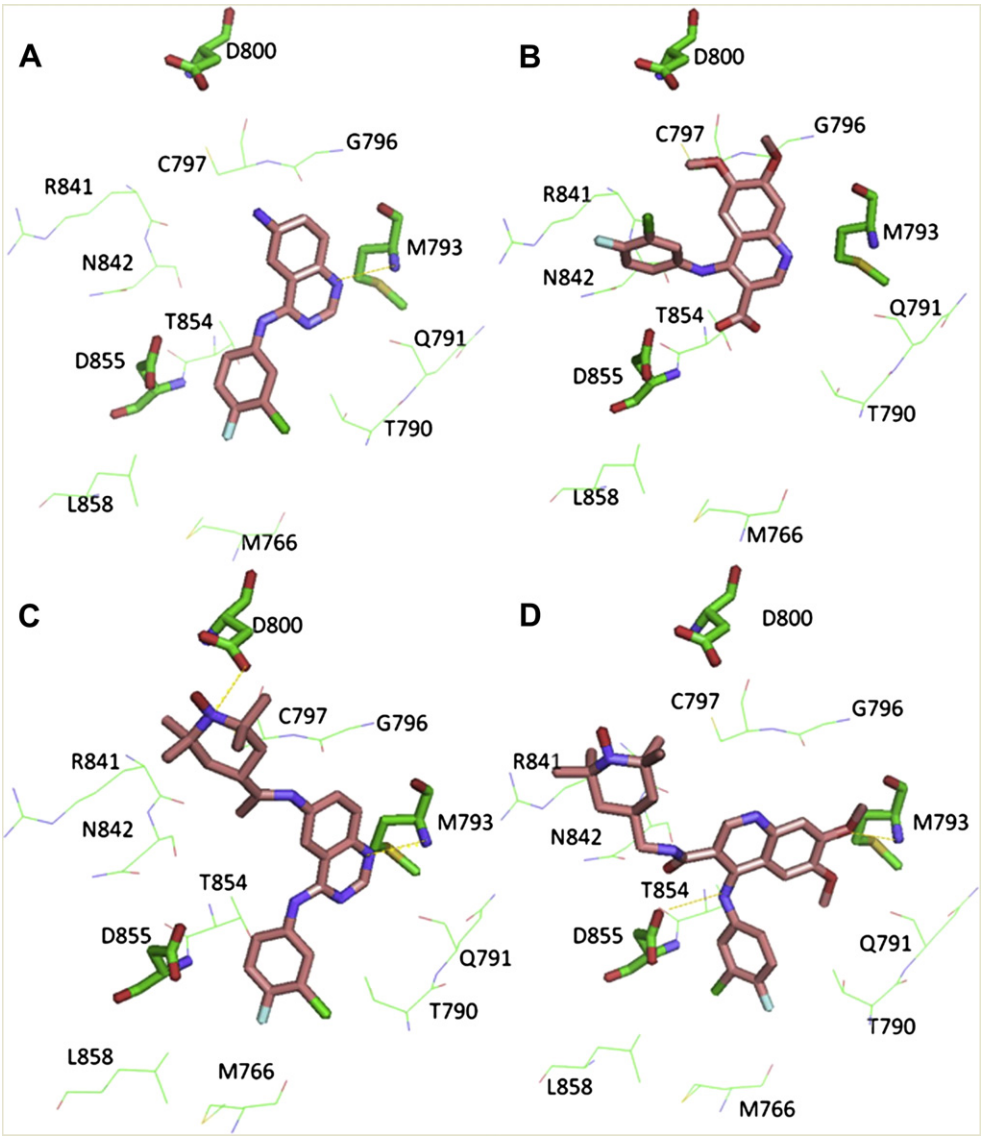

Fig. 4. Compound **1c**, **2c**, **3c** and **4c** binding to the ATP-binding pocket of EGFR. The carbon in EGFR was colored in green, ligand carbons were colored in pink. The important residues in EGFR and all the ligands were represented with the sticks style. Hydrogen bonds were represented with yellow discontinuous line. The left top sign A, B, C and D corresponding to compounds **1c**, **2c**, **3c** and **4c**, respectively. All graphical pictures were made using the Pymol program. (For interpretation of the references to colour in this figure legend, the reader is referred to the web version of this article.)

cellular and the molecular experimental data. The model will be helpful for our further structural elaboration of the novel TEMPO beard EGFR inhibitors.

4. Conclusion

In this paper, we synthesized a series of 4-anilinoquinazoline and 4-anilinoquinoline derivatives bearing a TEMPO. We also evaluated these compounds and their corresponding parent compounds in vitro with EGFR tyrosine kinase and A431 cell lines. All of the compounds bearing TEMPO showed more favorable effect than their parent compounds in EGFR kinase assay and anti-proliferative assay. Among of them, series **3** showed the higher potency to EGFR kinase. Furthermore, we have proved that inhibitor bearing a TEMPO can enter cells to exert inhibitory effect. It is concluded that inhibitor bearing TEMPO can increase anti-proliferative potency against A431 cells, such as series **3** which are more favorable to be EGFR inhibitors and can possibly be used for EPR spin labeling of EGFR overexpressing cancers as a bio-probe agent. Further work will be focused on improving cell membrane permeability of these TEMPO-derived analogues.

5. Experimental

5.1. Chemistry

Melting points were determined in open capillary tubes on an SGW X-4 micro melting point apparatus and were uncorrected. Electron impact and high-resolution mass spectra were obtained on a Micromass GCT spectrometer. Infrared spectra were recorded on a Nicolet FT-IR series using KBr cell. Conventional ^{1}H NMR spectra of nitroxide-containing molecules are quite broad which are not used for identify the molecular structure during a chemical synthesis [29], while ^{13}C NMR spectra are sufficiently legible and used by researchers [30]. ^{13}C NMR spectra were measured on Brucker 400 MHz in δ scale. The spectra were

obtained with solutions of DMSO-d_6 or CH_3OH-d_4 with TMS as internal standard, and the values of the chemical shifts (δ) were given in ppm. Elemental analyses were carried out at VARIO ELIII apparatus.

*5.1.1. General procedures for the synthesis of **3a–c***

To a stirred solution of **1a** (1.00 g, 3.70 mmol) and 4-carboxy-2,2,6,6-tetramethylpiperidine-N-oxyl (**4-COOH-TEMPO**) (1.48 g, 7.40 mmol) in 150 mL dichloromethane at 0 °C, tetrahydrofunan solution 50 mL containing HOBt (1.00 g, 7.40 mmol) was added. After being stirred at 0 °C for 30 min, EDC (1.42 g, 7.40 mmol) was added. Then the temperature of the reaction warmed to room temperature naturally, and the reaction mixture was kept stirring overnight before evaporating under reduced pressure. The residue dissolved in 200 mL chloroform, was rinsed three times with $NaHCO_3$ saturated solution, when the organic layer dried over anhydrous $MgSO_4$, the solvent removed. The crude material was purified by silica gel chromatography (eluent $CH_3CO_2C_2H_5$:THF = 5:2), and generated pure desired product.

*5.1.1.1. 2,2,6,6-Tetramethyl-1-oxyl-N-[4-(3-chlorophenylamino)quinazolin-6-yl]piperidine-4-carboxamide (**3a**).* Red solid, 23% yield. mp 206–208 °C. IR (KBr) cm^{-1} 3282(NH), 3199 3144 3087 3065 (NH, acylamide), 2977(CH_3), 2926(CH_2), 1694(CO), 1363(NO). ^{13}C NMR (400 MHz, DMSO-d_6): δ 157.4, 154.2, 146.8, 141.2, 137.8, 133.0, 131.0, 129.3, 127.8, 124.0, 121.9, 120.9, 115.6, 112.2. HRMS for $C_{24}H_{27}N_5O_2Cl$, Calcd: 452.1853, Found: 452.1855. Anal. Calc. for $C_{24}H_{27}ClN_5O_2$: C, 63.64; H, 6.01; N, 15.46. Found: C, 63.52; H, 5.63; N, 15.12.

*5.1.1.2. 2,2,6,6-Tetramethyl-1-oxyl-N-[4-(3-bromophenylamino)quinazolin-6- yl]piperidine-4-carboxamide (**3b**).* Red solid, 30% yield. mp 216–218 °C. IR (KBr) cm^{-1} 3281(NH), 3241 3143 3085 3040(NH, acylamide), 2974(CH_3), 2928(CH_2), 1693(CO), 1362(NO). ^{13}C NMR (400 MHz, DMSO-d_6): δ 157.3, 154.0, 146.8, 141.3, 137.8, 131.2, 129.1, 127.7, 126.7, 124.7, 121.8, 121.4, 115.6, 112.1. HRMS for $C_{24}H_{27}N_5O_2Br$, Calcd: 496.1348, Found: 496.1349. Anal. Calc. for $C_{24}H_{27}BrN_5O_2$: C, 57.95; H, 5.47; N, 14.08. Found: C, 57.83; H, 5.51; N,13.87.

*5.1.1.3. 2,2,6,6-Tetramethyl-1-oxyl-N-[4-(3-chloro-4-fluorophenylamino) quinazolin-6-yl]piperidine-4-carboxamide (**3c**).* Red solid, 18% yield. mp 200–202 °C. IR (KBr) cm^{-1} 3531(NH), 3433 3331 3213 3108(NH, acylamide), 2978(CH_3), 2935(CH_2), 1661(CO), 1366(NO). ^{13}C NMR (400 MHz, DMSO-d_6): δ 157.3, 153.9, 152.1, 146.6, 137.7, 136.8, 129.1, 127.6, 124.1, 122.9, 119.0, 117.5, 115.4, 111.9. HRMS for $C_{24}H_{27}N_5O_2FCl$ (M + H), Calcd: 473.1808, Found: 473.1825. Anal. Calc. for $C_{24}H_{26}ClFN_5O_2$: C, 61.21; H, 5.56; N, 14.87. Found: C, 61.01; H,5.89; N,14.56.

*5.1.2. General procedures for the synthesis of **4a–c***

The synthesis of **4a–c** was performed using similar protocols for the synthesis of **3a–c** except using appropriate 4-anilinoquinoline and 4-amino-2,2,6,6-tetramethylpiperidine-N-oxyl (**4-NH$_2$-TEMPO**) instead of appropriate 4-anilinoquinazoline and 4-carboxy-2,2,6,6-tetramethylpiperidine-N-oxyl (**4-COOH-TEMPO**).

*5.1.2.1. 4-(3-Chlorophenylamino)-6,7-dimethoxy-N-[(2,2,6,6-tetramethyl-1-oxyl)piperidin-4-yl]quinoline-3-carboxamide (**4a**).* Pink solid, 15% yield. mp 139–141 °C. IR (KBr) cm^{-1} 3282(NH), 3065(NH, acylamide), 2969(CH_3), 2931(CH_2), 1628(CO), 1365(NO). ^{13}C NMR (400 MHz, DMSO-d_6): δ 152.6, 148.9, 148.1, 146.5, 145.2, 142.9, 133.3, 130.6, 120.9, 120.8, 117.9, 116.6, 116.3, 108.3, 102.3, 56.2, 56.1. HRMS for $C_{27}H_{32}N_4O_4Cl$, Calcd: 511.2112, Found: 511.2122. Anal. Calc. for $C_{27}H_{32}ClN_4O_4$: C, 63.34; H, 6.30; N, 10.94. Found: C, 63.01; H, 6.49; N, 11.12.

*5.1.2.2. 4-(3-Bromophenylamino)-6,7-dimethoxy-N-[(2,2,6,6-tetramethyl-1-oxyl)piperidin-4-yl]quinoline-3-carboxamide (**4b**).* Pink solid, 17% yield. mp 138–140 °C. IR (KBr) cm^{-1} 3362(NH), 3325 3062(NH, acylamide), 2975(CH_3), 2931(CH_2), 1628(CO), 1365(NO). ^{13}C NMR (400 MHz, CH_3OH-d_4): δ 155.2, 151.2, 148.8, 147.6, 146.4, 146.0, 131.9, 126.3, 123.7, 123.3, 119.0, 118.0, 108.1, 103.3, 56.8. HRMS for $C_{27}H_{32}N_4O_4Br$, Calcd: 555.1607, Found: 555.1625. Anal. Calc. for $C_{27}H_{32}BrN_4O_4$: C, 58.28; H, 5.80; N, 10.07. Found: C, 57.98; H, 5.51; N, 9.89.

*5.1.2.3. 4-(3-Chloro-4-fluorophenylamino)-6,7-dimethoxy-N-[(2,2,6,6-tetramethyl-1-oxyl)piperidin-4-yl]quinoline-3-carboxamide (**4c**).* Pink solid, 12% yield. mp 148–150 °C. IR (KBr) cm^{-1} 3336(NH), 3066(NH, acylamide), 2973(CH_3), 2934(CH_2), 1624(CO), 1368(NO). ^{13}C NMR (400 MHz, CH_3OH-d_4): δ 155.2, 151.2, 148.8, 147.5, 146.7, 141.8, 123.0, 121.4, 117.6, 108.1, 103.1, 56.8. HRMS for $C_{27}H_{32}N_4O_4FCl$ (M + H), Calcd: 530.2096, Found: 530.2103. Anal. Calc. for $C_{27}H_{31}ClFN_4O_4$: C, 61.19; H, 5.90; N, 10.57. Found: C, 61.46; H, 6.11; N, 10.52.

5.2. Kinase assay

The kinase inhibition assay and IC_{50} determinations for wild type EGFR were measured with the homogeneous time-resolved fluorescence (HTRF) KinEASE-TK assay from Cisbio according to the manufacturer's instructions. Wild type EGFR was purchased from Carna Biosciences and 0.09 ng/μL kinase were used for test. ATP concentration were set at its K_m values (23 μM), and 180 nM substrate were used. Kinase, substrate peptide and inhibitors were added in 384 well plate, and then reaction was started by addition of ATP. After completion of the reaction (50 min later), an anti-phosphotyrosine antibody labeled with europium cryptate and streptavidin labeled with the fluorophore XL665 were added. The FRET between europium cryptate and XL665 was measured to quantify the phosphorylation of the substrate peptide. A Tecan i-control infinite 500 was used to measure the fluorescence of the samples at 620 nm (Eu-labeled antibody) and 665 nm (XL665 labeled streptavidin) 500 μs after excition at 320 nm. The quotient of both intensities for reactions made with ten different inhibitor concentrations (0.01 nM–10 μM, including no inhibitor) was plotted against inhibitor concentrations to determine IC_{50} values. Each reaction was performed in duplicate, and at least two independent determinations of each IC_{50} were made.

5.3. Biology. In vitro evaluation assay

Human epidermoid carcinoma (A431) cells were routinely grown at 37 °C in a humidified incubator with 5% CO_2 in DMEM medium supplemented with 10% fetal bovine serum (FBS), 2 mM glutamine, 50 U/mL penicillin and 50 μg/mL streptomycin. To determine the cell proliferation, the A431 cells were seeded in 96-well plates at 1×10^4 cells/well. All experiments were performed after 24 h of incubation at 37 °C in 5% CO_2.

The cell proliferation was evaluated with the MTT(3-(4,5-dimethyl-2-thiazolyl)-2,5-diphenyl-2H-tetrazolium bromide) assay, as described by Mosmann [31]. Briefly, A431 cells were treated with compounds (0.1–100 μM) for 72 h at 37 °C in 5% CO_2. After that, the cells were washed with phosphate buffered saline (PBS) and then incubated with MTT (5 mg/mL) in DMEM medium for 4 h. After removal of MTT and further washing, the formazan crystals were dissolved with DMSO. The amount of formazan was measured (492 nm, 630 nm) with a spectrophotometer.

The cell viability was expressed as percentage of control cells and calculated by the formula $F_t/F_{nt} \times 100$, where F_t = absorbance of treated cells and F_{nt} = absorbance of untreated cells. At least three independent dose–response curves were done and the

concentration of compound resulting in 50% inhibition of cell proliferation (IC_{50}) was calculated.

5.4. EPR detecting

To prove compounds **3c** and **4c** can get into cells, we detected EPR signals of intracellular **3c** and **4c**. In this test, we chose A431 cell lines as cell model same as MTT assays. Concisely, A431 cells were seeded in 6-well plates at 1×10^6 cells/well. After 24 h, the cells were treated with 20 μM **3c** and **4c**, respectively. 8 h later, compounds were removed from medium. Cells were washed with D-Hanks (contain 1%DMSO) completely until no EPR signals detected from the D-Hanks. 200 μL DMSO was added in each well and then undertook detection of EPR signals of DMSO solution after the DMSO dissolved cells.

EPR measurements were carried out by transferring DMSO solution containing cells to gas-permeable soft capillary tube. Each capillary was folded once, inserted into a narrow quartz tube (2.5 mm inner diameter) which was open at one end, and then placed in the EPR cavity. EPR parameters are as follows: modulation amplitude, 0.8 G; time constant, 0.164 s; sweep time, 20.972 s; modulation frequency, 100 kHz; and microwave power, 4.010 mW.

5.5. Docking study

Crystal structure of EGFR was downloaded from the PDB database (PDB ID: 1XKK) [32]. There were five missing loops (ML1-ML5) in the crystal structure. In order to patch the missing loops, the other three structures (PDB ID: 2ITT, 2ITO, 2GS6) were also downloaded from the PDB database. With the three structures, the ML1-ML5 were copied to 1XKK. ML1 (^{734}EGEK^{737}) and ML2 (^{750}ATSP^{753}) were modeled from 2ITT. 2GS6, which was a complex of EGFR/ATP, was used to model the ML3 (^{868}EYHAEGGK^{875}). The left missing residues (^{988}HLPSPTD^{994}) and (^{1005}EDMDD^{1009}) were built from 2ITO. To build the loops, crystal structure 2ITT, 2GS6, 2ITO were aligned to the 1XKK in Maestro and the corresponding regions were adopted for the missing residues in 1XKK, following with 500 iterations minimization with Macromodel on the affected regions while holding the remaining residues fixed. Finally, the fixed protein structure was prepared with the Protein Preparation Wizard [33]. This step involved setting correct bond orders, adding hydrogen, reorienting various groups and varying residue protonation states to optimize the hydrogen bonding network. With respect to the ligands, LigPrep [34] was employed to prepare all of them. All the possible protonation states at pH 5–9 for the compounds were generated with Epik in this procedure. The docking programs did not support docking compounds with free radical, such as the compounds series **3** and **4**. The non-radical forms of the ligands (ring-O^{-1} and ring-OH) were used in this simulation. Although the electrostatics would be a bit different, it did not exert big influence on the docking result.

Glide 5.5 was used to dock the twelve compounds into the binding pocket. The accuracy of this procedure was set to standard precise (SP). At first, grid file was generated with the ligand in 1XKK as the locator. Secondly, the ligands were docked into the pocket flexibly. To soften the potential for nonpolar parts of the ligand, the vdW radii of the ligand atoms were scalled with a factor of 0.8. Post-docking minimization was also performed to generate the better binding poses. At last, 5 poses of the ligands were obtained with the other parametres set as default.

Acknowledgements

This work was supported by the Science and Technology Commission of Shanghai Municipality (STCSM, No. 10dz2220500 and No. 09520703200) and the National Special Fund for State Key Laboratory of Bioreactor Engineering (No. 2060204).

References

[1] A. Antonello, A. Tarozzi, F. Morroni, A. Cavalli, M. Rosini, P. Hrelia, M.L. Bolognesi, C. Melchiorre, Multitarget-directed drug design strategy: a novel molecule designed to block epidermal growth factor receptor (EGFR) and to exert proapoptotic effects, J. Med. Chem. 49 (2006) 6642–6645.
[2] Z. Rachid, F. Brahimi, Q. Qiu, C. Williams, J.M. Hartley, J.A. Hartley, B.J. Jean-Claude, Novel nitrogen mustard-armed combi-molecules for the selective targeting of epidermal growth factor receptor overexperessing solid tumors: discovery of an unusual structure-activity relationship, J. Med. Chem. 50 (2007) 2605–2608.
[3] S. Bishayee, Role of conformational alteration in the epidermal growth factor receptor (EGFR) function, Biochem. Pharmacol. 60 (2000) 1217–1223.
[4] H. Ogiso, R. Ishitani, O. Nureki, S. Fukai, M. Yamanaka, J.-H. Kim, K. Saito, A. Sakamoto, M. Inoue, M. Shirouzu, S. Yokoyama, Crystal structure of the complex of human epidermal growth factor and receptor extracellular domains, Cell 110 (2002) 775–787.
[5] T. Holbro, G. Civenni, N.E. Hynes, The ErbB receptors and their role in cancer progression, Exp. Cell Res. 284 (2003) 99–110.
[6] N. Hynes, K. Horsch, M. Olayioye, A. Badache, The ErbB receptor tyrosine family as signal integrators, Endocr. Relat. Cancer 8 (2001) 151–159.
[7] C. Kuan, C. Wikstrand, D. Bigner, EGF mutant receptor vIII as a molecular target in cancer therapy, Endocr. Relat. Cancer 8 (2001) 83–96.
[8] Y. Umekita, Y. Ohi, Y. Sagara, H. Yoshida, Co-expression of epidermal growth factor receptor and transforming growth factor-alpha predicts worse prognosis in breast-cancer patients, Int. J. Cancer 89 (2000) 484–487.
[9] F.R. Hirsch, M. Varella-Garcia, P.A. Bunn Jr., M.V. Di Maria, R. Veve, R.M. Bremnes, A.E. Baron, C. Zeng, W.A. Franklin, Epidermal growth factor receptor in non-small-cell lung carcinomas: correlation between gene copy number and protein expression and impact on prognosis, J. Clin. Oncol. 21 (2003) 3798–3807.
[10] B. Biersack, M. Zoldakova, K. Effenberger, R. Schobert, (Arene)Ru(II) complexes of epidermal growth factor receptor inhibiting tyrphostins with enhanced selectivity and cytotoxicity in cancer cells, Eur. J. Med. Chem. 45 (2010) 1972–1975.
[11] A. Bourkoula, M. Paravatou-Petsotas, A. Papadopoulos, I. Santos, H.-J. Pietzsch, E. Livaniou, M. Pelecanou, M. Papadopoulos, I. Pirmettis, Synthesis and characterization of rhenium and technetium-99m tricarbonyl complexes bearing the 4-[3-bromophenyl]quinazoline moiety as a biomarker for EGFR-TK imaging, Eur. J. Med. Chem. 44 (2009) 4021–4027.
[12] T. Fozing, C. Scheuer, S. Samnick, Synthesis and initial tumor affinity testing of iodine-123 labelled EGFR-affine agents as potential imaging probes for hormone-refractory prostate cancer, Eur. J. Med. Chem. 45 (2010) 3780–3786.
[13] J. Domarkas, F. Dudouit, C. Williams, Q. Qiyu, R. Banerjee, F. Brahimi, B.J. Jean-Claude, The combi-targeting concept: synthesis of stable nitrosoureas designed to inhibit the epidermal growth factor receptor (EGFR), J. Med. Chem. 49 (2006) 3544–3552.
[14] M.B. Gariboldi, S. Lucchi, C. Caserini, R. Supino, C. Oliva, E. Monti, Antiproliferative effect of the piperidine nitroxide tempol on neoplastic and non-neoplastic mammalian cell lines, Free Radic. Biol. Med. 24 (1998) 913–923.
[15] M.B. Gariboldi, R. Ravizza, C. Petterino, M. Castagnaro, G. Finocchiaro, E. Monti, Study of in vitro and in vivo effects of the piperidine nitroxide Tempol–a potential new therapeutic agent for gliomas, Eur. J. Cancer 39 (2003) 829–837.
[16] M.B. Gariboldi, V. Rimoldi, R. Supino, E. Favini, E. Monti, The nitroxide tempol induces oxidative stress, p21WAF1/CIP1, and cell death in HL60 cells, Free Radic. Biol. Med. 29 (2000) 633–641.
[17] E. Monti, R. Supino, M. Colleoni, B. Costa, R. Ravizza, M.B. Gariboldi, Nitroxide TEMPOL impairs mitochondrial function and induces apoptosis in HL60 cells, J. Cell. Biochem. 82 (2001) 271–276.
[18] F. Hyodo, K.-i Matsumoto, A. Matsumoto, J.B. Mitchell, M.C. Krishna, Probing the intracellular redox status of tumors with magnetic resonance imaging and redox-sensitive contrast agents, Cancer Res. 66 (2006) 9921–9928.
[19] P. Kuppusamy, M. Afeworki, R.A. Shankar, D. Coffin, M.C. Krishna, S.M. Hahn, J.B. Mitchell, J.L. Zweier, In vivo electron paramagnetic resonance imaging of tumor heterogeneity and oxygenation in a murine model, Cancer Res. 58 (1998) 1562–1568.
[20] K.-i. Matsumoto, F. Hyodo, A. Matsumoto, A.P. Koretsky, A.L. Sowers, J.B. Mitchell, M.C. Krishna, High-resolution mapping of tumor redox status by magnetic resonance imaging using nitroxides as redox-sensitive contrast agents, Clin. Cancer Res. 12 (2006) 2455–2462.
[21] H.-R. Tsou, N. Mamuya, B.D. Johnson, M.F. Reich, B.C. Gruber, F. Ye, R. Nilakantan, R. Shen, C. Discafani, R. DeBlanc, R. Davis, F.E. Koehn, L.M. Greenberger, Y.-F. Wang, A. Wissner, 6-Substituted-4-(3-bromophenylamino)quinazolines as putative irreversible inhibitors of the epidermal growth factor receptor (EGFR) and human epidermal growth factor receptor (HER-2) tyrosine kinases with enhanced antitumor activity, J. Med. Chem. 44 (2001) 2719–2734.
[22] A. Wissner, D.M. Berger, D.H. Boschelli, M.B. Floyd, L.M. Greenberger, B.C. Gruber, B.D. Johnson, N. Mamuya, R. Nilakantan, M.F. Reich, R. Shen, H.-

R. Tsou, E. Upeslacis, Y.F. Wang, B. Wu, F. Ye, N. Zhang, 4-Anilino-6,7-dialkoxyquinoline-3-carbonitrile inhibitors of epidermal growth factor receptor kinase and their bioisosteric relationship to the 4-anilino-6,7-dialkoxyquinazoline inhibitors, J. Med. Chem. 43 (2000) 3244–3256.

[23] S.R. Klutchko, H. Zhou, R.T. Winters, T.P. Tran, A.J. Bridges, I.W. Althaus, D.M. Amato, W.L. Elliott, P.A. Ellis, M.A. Meade, Tyrosine kinase inhibitors. 19. 6-Alkynamides of 4-anilinoquinazolines and 4-anilinopyrido [3, 4-d] pyrimidines as irreversible inhibitors of the erbB family of tyrosine kinase receptors, J. Med. Chem. 49 (2006) 1475–1485.

[24] C. Fernandes, C. Oliveira, L. Gano, A. Bourkoula, I. Pirmettis, I. Santos, Radioiodination of new EGFR inhibitors as potential SPECT agents for molecular imaging of breast cancer, Bioorg. Med. Chem. 15 (2007) 3974–3980.

[25] A.M. Samuni, W. DeGraff, M.C. Krishna, J.B. Mitchell, Cellular sites of H_2O_2-induced damage and their protection by nitroxides, Biochim. Biophys. Acta (BBA). Gen. Subjects 1525 (2001) 70–76.

[26] E.R. Wood, A.T. Truesdale, O.B. McDonald, D. Yuan, A. Hassell, S.H. Dickerson, B. Ellis, C. Pennisi, E. Horne, K. Lackey, K.J. Alligood, D.W. Rusnak, T.M. Gilmer, L. Shewchuk, A unique structure for epidermal growth factor receptor bound to GW572016 (Lapatinib), Cancer Res. 64 (2004) 6652–6659.

[27] J. Stamos, M.X. Sliwkowski, C. Eigenbrot, Structure of the epidermal growth factor receptor kinase domain alone and in complex with a 4-anilinoquinazoline inhibitor, J. Biol. Chem. 277 (2002) 46265–46272.

[28] C.-H. Yun, T.J. Boggon, Y. Li, M.S. Woo, H. Greulich, M. Meyerson, M.J. Eck, Structures of lung cancer-derived EGFR mutants and inhibitor complexes: mechanism of activation and insights into differential inhibitor sensitivity, Cancer Cell 11 (2007) 217–227.

[29] J.F.W. Keana, Newer aspects of the synthesis and chemistry of nitroxide spin labels, Chem. Rev. 78 (1978) 37–64.

[30] C.E. Müller, R. Hrdina, R.C. Wende, P.R. Schreiner, A multicatalyst system for the one-pot desymmetrization/oxidation of meso-1,2-alkane diols, Chem. Eur. J. 17 (2011) 6309–6314.

[31] T. Mosmann, Rapid colorimetric assay for cellular growth and survival: application to proliferation and cytotoxicity assays, J. Immunol. Methods 65 (1983) 55–63.

[32] H.M. Berman, J. Westbrook, Z. Feng, G. Gilliland, T.N. Bhat, H. Weissig, I.N. Shindyalov, P.E. Bourne, The protein data Bank, Nucleic Acids Res. 28 (2000) 235–242.

[33] Maestro, Schrödinger, LLC, New York, NY, 2008.

[34] Ligprep, Schrödinger, LLC, New York, NY, 2008.